Available online at www.sciencedirect.com
ScienceDirect
Phytochemistry 68 (2007) 1189–1199
PHYTOCHEMISTRY
www.elsevier.com/locate/phytochem

Constituents from the Formosan apple reduce tyrosinase activity in human epidermal melanocytes

Yi-Pei Lin [a], Feng-Lin Hsu [a], Chien-Shu Chen [b], Ji-Wang Chern [b], Mei-Hsien Lee [b,*]

[a] *Graduate Institute of Pharmacognosy, College of Pharmacy, Taipei Medical University, 250 Wu Hsing Street, Taipei 110, Taiwan*
[b] *School of Pharmacy, College of Medicine, National Taiwan University, Taipei 100, Taiwan*

Received 30 June 2006; received in revised form 9 January 2007
Available online 26 March 2007

Abstract

Tyrosinase is a copper-containing monooxygenase that catalyzes melanin synthesis in skin melanocytes. Herein, 13 compounds from the Formosan apple (*Malus doumeri* var. *formosana*), an indigenous Taiwanese plant, were isolated and identified. The active constituents were identified as 3-hydroxyphloretin (**7**) and catechol (**9**); they exhibited potent hydroxyl radical-scavenging (IC_{50} values, 0.6 and 1.1 μM) and cellular tyrosinase-reducing activities (IC_{50} values, 32 and 22 μM) in human epidermal melanocytes. In addition, we evaluated the level of several tyrosinase-related proteins by Western blot analysis. In contrast to 3-hydroxyphloretin (**7**), which showed no effect on the level of these proteins, catechol (**9**) reduced their activity and the expression of the respective genes, as determined by quantitative real-time PCR. In a kinetic analysis of mushroom tyrosinase, 3-hydroxyphloretin (**7**) was a competitive inhibitor. These two constituents exhibited metal-coordinating interactions with copper ions in a virtual model of molecular docking with human tyrosinase. Thus, 3-hydroxyphloretin (**7**) and catechol (**9**) were the most active constituents from the Formosan apple; they exhibited anti-oxidant and tyrosinase reducing activities, suggesting their possible use as cosmetic agents.

Keywords: Formosan apple; *Malus doumeri* var. *formosana*; Rosaceae; 3-Hydroxyphloretin; Catechol; Tyrosinase; Human epidermal melanocytes; Quantitative real-time PCR; Molecular docking

1. Introduction

Tyrosinase (EC 1.14.18.1) is widely distributed among various organisms and is important for browning in plants. Tyrosinase activity also induces undesirable browning in cut fruits, vegetables, and beverages; this is a major problem in the food industry. Tyrosinases are not only involved in the induction of browning in plants but also in melanization in animals. Pigment synthesis involves the conversion of tyrosine to melanin, and tyrosinases catalyze the rate-limiting step of melanin synthesis in melanocytes. Many reports describe pharmacologic and cosmetic agents that inhibit tyrosinase activity or that block melanogenic pathways, leading to skin lightening (Kim and Uyama, 2005). Tyrosinases catalyze two distinct reactions in melanin synthesis: the hydroxylation of tyrosine to 3,4-dihydroxyphenylalanine (DOPA) and the oxidation of DOPA to dopaquinone (Tripathi et al., 1992). After spontaneous conversion of dopaquinone to dopachrome, dopachrome tautomerase (tyrosinase-related protein-2, DCT/TRP-2) catalyzes the conversion of dopachrome to 5,6-dihydroxyindole-2-carboxylic acid (DHICA). Subsequently, DHICA is converted to indole–quinone–carboxylic acid by DHICA oxidase (tyrosinase-related protein-1, TRP-1) (Maeda et al., 1997). In general, the activity of tyrosinase and the protein levels of tyrosinase, TRP-1, and TRP-2 correlate directly with melanin content. It was shown that melanocytes derived from pale skin, with a low melanin content, consistently have lower tyrosinase activity and levels of tyrosinase, TRP-1, and TRP-2 than melanocytes derived from darker skin, with a higher mela-

* Corresponding author. Tel.: +886 2 2736 1661x6151.
E-mail address: Lmh@tmu.edu.tw (M.-H. Lee).

0031-9422/$ - see front matter © 2007 Elsevier Ltd. All rights reserved.
doi:10.1016/j.phytochem.2007.02.001

nin content (Halaban et al., 1983; Abdel-Malek et al., 1993, 1994). The tyrosinase-related proteins, TRP-1, and DCT/TRP-2 catalyze distal melanin biosynthesis steps that control the type of melanin produced. In addition to their roles in pigmentation, tyrosinase family proteins also influence the biology of melanocytes (Sturm et al., 1998; Hirobe, 2005).

The human tyrosinase-related proteins (TYRPs) include the tyrosinase enzymes and a family of closely related melanocyte-specific gene products involved in melanin synthesis (Fang et al., 2002). The chromosomal locations of the loci that contain the three human *TYRP* genes have been determined and searches have been conducted for functional polymorphisms that could explain natural variation in pigmentation phenotypes and several hypopigmented states. Expression of tyrosinase and a family of related genes (i.e., *TYRP*1 and *TYRP*2) is the hallmark of cells of the mammalian melanocytic lineage (Hearing, 1999). Melanin biosynthesis can be inhibited by several methods, including avoiding UV exposure, inhibition of melanocyte metabolism and proliferation (Eberle et al., 2001; Yamakoshi et al., 2003), and the inhibition of tyrosinase. Recently, tyrosinase inhibitors have been used in cosmetic products that promote skin-whitening (Kadekaro et al., 2003a,b).

Formosan apple (*Malus doumeri* A. Chev. var. *formosana* (Kawak. & Koidz.) S.S. Ying, Rosaceae) is an indigenous Taiwanese plant. It has been used traditionally in Taiwan to treat heat-related hyperactivity and as a tonic (Kao, 1996). In a previous study, we found that there were several constituents in this plant that possess free radical-scavenging, anti-elastase, and anti-matrix metalloproteinase-1 (MMP-1) activity in human skin fibroblast cells (Leu et al., 2006). However, the medicinal effects of compounds from the Formosan apple on human epidermal melanocytes (HEMn) remained unclear. Here, we further purified and characterized several constituents from the Formosan apple. We evaluated their effects on melanin synthesis in HEMn cells using Western blot analyses of tyrosinase-related proteins, quantitative real-time PCR, and molecular docking models.

2. Results and discussion

2.1. Purification of constituents from Formosan apple

In a previous study, flavonoids (**1**)–(**7**) were isolated from Formosan apple and were shown to inhibit matrix metalloproteinases (MMPs) in human fibroblast cells (Leu et al., 2006). In addition to the previous seven compounds, in this study we further isolated the phenolic derivatives, protocatechuic acid (**8**) (An et al., 2006) and catechol (**9**) (Webb and Ruszkay, 1998), as well as the flavonol, rutin (**10**) (Hou et al., 2005) from an ethyl acetate extract. The stilbene, pynosylvin (**11**) (Schultz et al., 1992) and the triterpenoids, oleanolic acid (**12**) and ursolic acid (**13**) (Budzikiewicz et al., 1963) were isolated from the aqueous layer. Structural determinations were made by comparison of ^{1}H and ^{13}C NMR spectra with those reported in the literatures. Compounds (**8**)–(**13**) were isolated from Formosan apple for the first time; their chemical structures are presented in Fig. 1.

2.2. The effect of the Formosan apple constituents on hydroxyl radical-scavenging activity

Aging has been associated with free radical formation (Harman, 2003). Hydroxyl radicals are one of the most reactive radicals generated from biologic molecules and can damage living cells (Bergamini et al., 2004). It has been reported that some plant extracts can scavenge hydroxyl radicals and may protect cellular lipids against free radical reactions (Reiter et al., 2001). Phloretin (**1**), phloridzin (**2**), 3-hydroxyphlorizin (**3**), quercetin (**4**), chrysin (**5**), 3-hydroxyphloretin (**7**), protocatechuic acid (**8**), catechol (**9**), rutin (**10**), and pynosylvin (**11**) exhibit hydroxyl radical-scavenging activities, with IC_{50} values of 0.8, 87, 30, 1.2, 45, 0.6, 42, 1.1, 80, and 2.5 μM, respectively (Fig. 2). Trolox was used as a positive control; its IC_{50} value was 25 μM in this assay (Fig. 2). Compared with the positive control, phloretin (**1**), quercetin (**4**), 3-hydroxyphloretin (**7**), catechol (**9**), and pynosylvin (**11**) have the strongest hydroxyl radical-scavenging properties.

2.3. Cytotoxicity of constituents from the Formosan apple, assessed in HEMn cells

An assessment of the cytotoxic properties of the constituents isolated from the Formosan apple is obviously of importance if the components are to be considered for cosmetic or therapeutic purposes in humans. Each of the isolated constituents was examined separately at a relatively high concentration (100 μM) for effects on the survival of HEMn cells. Using the MTT assay, cells exposed to all test samples exhibited a viability >80% (Fig. 3) in a 24 h treatment, demonstrating that the isolated compounds were not or less toxic in HEMn cells.

2.4. The tyrosinase- and melanin-reducing activities of the constituents from Formosan apple in HEMn cells

Melanin is an important factor affecting mammalian skin color (Hearing, 2005). The proximal pathway of melanogenesis consists of the enzymatic oxidation of tyrosine or L-DOPA to its corresponding *o*-dopaquinone, a step catalyzed by tyrosinase. After multiple additional biosynthesis steps, further polymerization yields melanin (Kim and Uyama, 2005). In the present study, each constituents isolated from the Formosan apple was examined for its ability to inhibit cellular tyrosinase activity and to reduce cellular melanin content in HEMn cells (Table 1). 3-Hydroxyphloretin (**7**) (inhibition 73%) and catechol (**9**) (inhibition 78%) showed substantial cellular tyrosinase inhibitory activity at a concentration of 100 μM. Quercetin (**4**) (inhi-

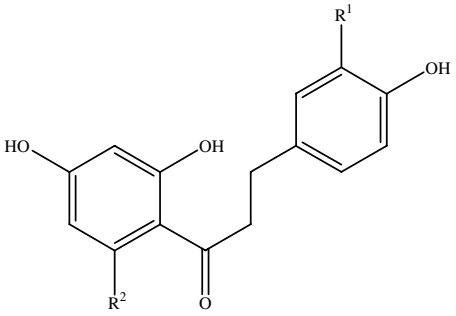

	R^1	R^2
Phloretin (**1**)	H	OH
Phloridzin (**2**)	H	OGlc
3-Hydroxyphloridzin (**3**)	OH	OGlc
3-Hydroxyphloretin (**7**)	OH	OH

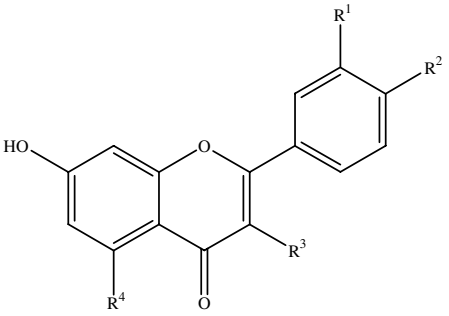

	R^1	R^2	R^3	R^4
Quercetin (**4**)	OH	OH	OH	OH
Chrysin (**5**)	H	H	H	OH
Chrysin-5-glucoside (**6**)	H	H	H	OGlc
Rutin (**10**)	OH	OH	Rutinoside	OH

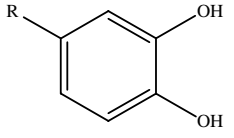

	R
Protocatechuic acid (**8**)	COOH
Catechol (**9**)	H

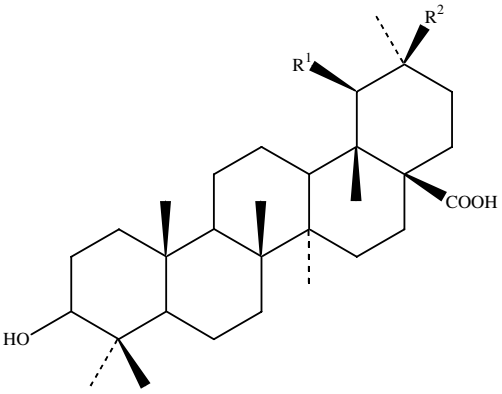

	R^1	R^2
Oleanolic acid (**12**)	H	CH_3
Ursolic acid (**13**)	CH_3	H

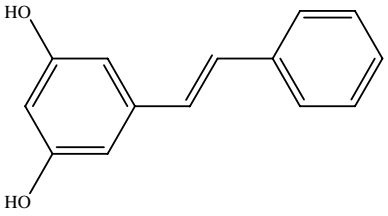

Pynosylvin (**11**)

Fig. 1. Schematic representation of the chemical structures of the isolated constituents from the Formosan apple.

bition 36%), protocatechuic acid (**8**) (inhibition 34%), and pynosylvin (**11**) (inhibition 32%) exhibited moderate inhibitory activity. Thus, 3-hydroxyphloretin (**7**) and catechol (**9**) were further evaluated for their anti-tyrosinase effects. As compared to treatment with medium only (untreated control), treatment with 3-hydroxyphloretin (**7**) and catechol (**9**) at concentrations ranging from 10 to 100 μM resulted in increasing degrees of reduction of tyrosinase in HEMn cells. The IC_{50} values of 3-hydroxyphloretin (**7**) and catechol (**9**) were 32 and 22 μM, respectively, in HEMn (Table 2). The commercially available depigmenting agent, arbutin, was used as a positive control ($IC_{50} = 3.0$ mM). Other supposed skin-whitening agents, vitamin C, ellagic acid, and hydroquinone, were also tested in our assay system. They exhibited less tyrosinase-inhibitory activity than 3-hydroxyphloretin (**7**) or catechol (**9**) (data not shown). Hydroquinone was also very toxic to HEMn; viability was greatly affected at a concentration of 20 μM. From

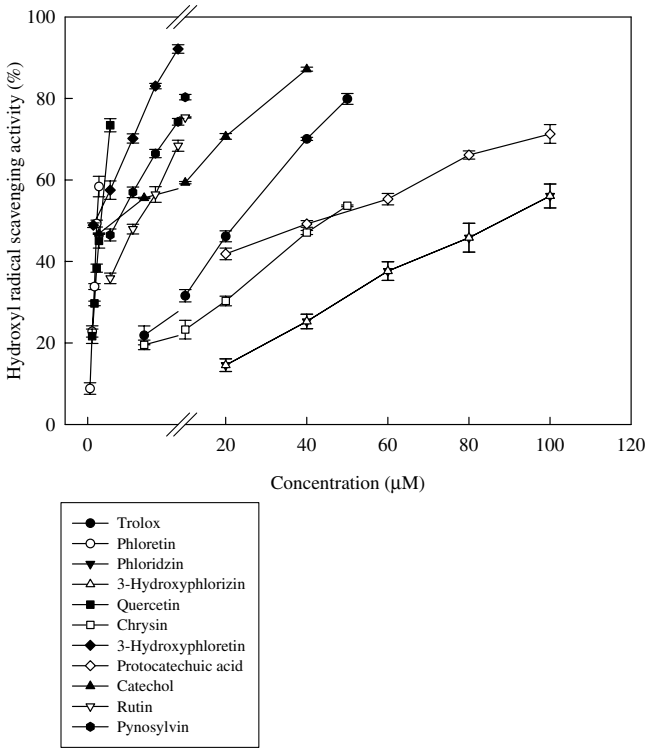

Fig. 2. The hydroxyl radical-scavenging activities of the constituents from the Formosan apple.

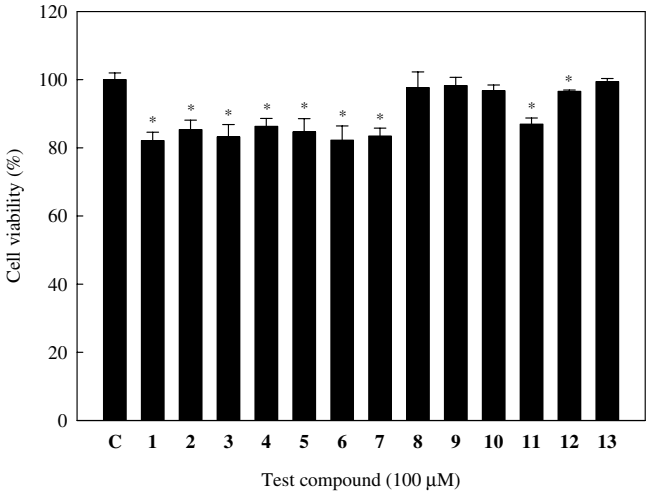

Fig. 3. The cell viabilities of the constituents from the Formosan apple in HEMn cells. Differences in data were evaluated for statistical significance ($p < 0.5$) using the non-parametric Mann–Whitney *U*-test.

the tyrosinase activity assay, we noticed that all active constituents contained the catechol skeleton in their chemical structure and that they all lacked sugar moieties. The catechol structure with two hydroxyl groups at the *o*-positions of the aromatic ring has been reported to bind copper ions and thus may compete with tyrosinase for available copper ions (Briganti et al., 2003; Khatib et al., 2005). Melanin is synthesized by a multi-step pathway. In addition to tyrosinase, melanin synthesis is controlled by TRP-1, TRP-2,

Table 1
Tyrosinase and melanin reduction by compounds isolated from the Formosan apple in HEMn cells

Compound (100 μM)	Reduction (mean ± SD), %	
	Cellular tyrosinase activity	Melanin content
Phloretin (**1**)	28.99 ± 3.57	9.15 ± 6.91
Phloridzin (**2**)	11.32 ± 2.34	–
3-Hydroxyphlorizin (**3**)	22.53 ± 2.33	–
Quercetin (**4**)	35.84 ± 2.94	7.36 ± 3.79
Chrysin (**5**)	22.96 ± 5.63	2.78 ± 8.35
Chrysin-5-glucoside (**6**)	16.64 ± 2.84	12.13 ± 6.54
3-Hydroxyphloretin (**7**)	80.50± 1.40	18.30 ± 4.90
Protocatechuic acid (**8**)	33.45 ± 1.59	–
Catechol (**9**)	78.13 ± 0.47	14.12 ± 3.91
Rutin (**10**)	16.94 ± 2.31	4.57 ± 3.10
Pynosylvin (**11**)	31.85 ± 1.92	2.19 ± 3.32
Oleanolic acid (**12**)	–	–
Ursolic acid (**13**)	–	–

"–" no effect.

and other factors, including UV exposure, prostaglandins, vitamins, growth factors, interleukins, interferons, and hormones (e.g., α-melanocyte-stimulating hormone (α-MSH), adrenocorticotropic hormone, and endothelin-1 (ET-1), melanotropin) (Fang et al., 2002; Kadekaro et al., 2003a,b; Parvez et al., 2006). Although both 3-hydroxyphloretin (**7**) and catechol (**9**) inhibited ~80% of tyrosinase activity (at 100 μM), they caused 17% and 2% reductions in cell viability, respectively, and had a marginal (~20%) reducing effect on melanin content. Furthermore, the reduction in melanin content by 3-hydroxyphloretin (**7**) may be due to the reduced cell viability.

2.5. Expression of genes encoding pigment-related proteins in the presence of 3-hydroxyphloretin (7) and catechol (9) in HEMn cells

The pigment-related proteins apparently behaved similarly to the pigment-related enzymes (Kushimoto et al., 2001, 2003). Expression of the corresponding genes following 24 h of treatment with 3-hydroxyphloretin (**7**) and catechol (**9**) were evaluated by Western blots at various concentrations of (**7**) and (**9**) (10, 25, 50, and 100 μM). For the three pigment-related proteins, 3-hydroxyphloretin (**7**) showed almost no effect on tyrosinase protein, TRP-1, or TRP-2 proteins at various doses (Fig. 4a). Catechol (**9**) showed a slight effect on the tyrosinase level at the various doses tested, almost no effect on the TRP-1 protein level, and a significant effect on the level of TRP-2 (Fig. 4b). The essential function of tyrosinase in melanin biosynthesis has been known for past six decades (Westerhof, 2006). In the absence of functional tyrosinase, no synthesis of melanin is observed in mammalian melanocytes (Hirobe, 2005). TRP-1 has been reported to play an important role in the stabilization of tyrosinase, has been demonstrated to be involved in the maintenance of melanosome ultrastructure, and affects melanocyte proliferation, morphology, and cell death (Vijayasaradhi et al., 1990, 1991;

Table 2
Tyrosinase and melanin reduction by arbutin, 3-hydroxyphloretin (**7**) and catechol (**9**)

Sample	Concentration (μM)	Tyrosinase reduction (%)	Melanin reduction (%)
Arbutin	500	29.8 ± 1.2	5.7 ± 0.1
	1000	36.0 ± 3.2	6.5 ± 1.2
	2500	43.5 ± 3.2	7.1 ± 2.0
	5000	67.1 ± 1.8	10.9 ± 1.7
3-Hydroxyphloretin (**7**)	10	1.4 ± 5.1	6.3 ± 2.9
	25	5.7 ± 1.7	18.9 ± 6.4
	50	43.9 ± 2.8	14. 7 ± 5.4
	100	80.5 ± 1.4	18.3 ± 4.9
Catechol (**9**)	10	42.0 ± 2.5	1.1 ± 3.6
	25	51.9 ± 2.8	18.3 ± 3.4
	50	65.8 ± 2.7	20.8 ± 2.7
	100	78.1 ± 0.5	14.1 ± 3.9

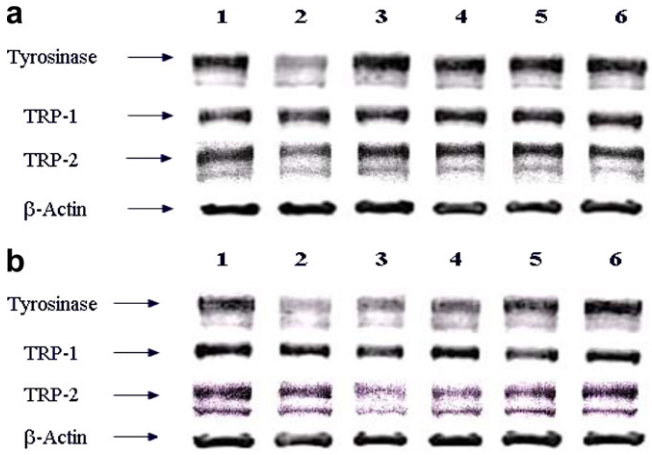

Fig. 4. Expression of genes encoding tyrosinase, TRP1, and TRP2/DCT in (a) 3-hydroxyphloretin (**7**) and (b) catechol (**9**)-treated human epidermal melanocytes (HEMn). Cultured melanocytes were treated with medium or test compounds for 24 h. Cells were then harvested and lysates (equal amount proteins) were subjected to polyacrylamide gel (10%) electrophoresis, followed by electroblotting and immunostaining with antibodies to tyrosinase, TRP1, and TRP2/DCT. 1, medium only; 2, arbutin (3.0 mM); 3, 100 μM; 4, 50 μM; 5, 25 μM; 6, 10 μM.

Houghton, 1994; Li et al., 2004). The presence of DCT/TRP-2 is thought to have implications for the cytotoxicity of melanogenic intermediates to melanocytes (Hearing, 2005). It is another important regulator in the pigment biosynthesis pathway (Widlund and Fisher, 2003). These proteins belong to a family of membrane proteins that are structurally related, but that have distinct enzymatic functions (Negroiu et al., 2000). Our results indicate that 3-hydroxyphloretin (**7**) exhibited tyrosinase-reducing activity, but did not affect tyrosinase-related proteins. It may interact with tyrosinase itself or compete for binding of the copper ions with the catalytic domain of tyrosinase, thereby reducing tyrosinase activity (Khatib et al., 2005; Kim et al., 2006). Catechol (**9**) influenced the expression of the tyrosinase- and TRP-2- encoding genes. The inhibitory effect of catechol (**9**) on melanin synthesis at 50 and 100 μM may involve a direct effect on particular steps of the melanin biosynthesis pathway.

2.6. Expression of tyrosinase-related genes in catechol-treated HEMn cells

To examine whether decreased transcription of the *TYR* and *TYRP2* genes was responsible for the observed decrease in expression of tyrosinase and DCT/TRP-2 in catechol (**9**)-treated HEMn cells, the levels of mRNAs encoding these proteins were assessed, using qRT-PCR. The gene for GAPDH served as a housekeeping gene control. The expression of the tyrosinase- and TRP2/DCT-encoding genes was found to be down-regulated in the presence of catechol (**9**) at 50 and 100 μM. As compared with the untreated control values, expression ratios were 1.9, 1.3, 0.9, and 0. 7 for the *TYR* gene and 2.4, 1.7, 0.4, and 0.2 for the *TYRP2* gene at concentrations of 10, 25, 50, and 100 μM catechol (**9**), respectively (Fig. 5). Catechol (**9**) may operate by different mechanisms at different concentrations. We found that the levels of *TYR* and *TYRP2* mRNA were increased at concentrations of 10 and 25 μM. This may be due to transcriptional activators (Oetting, 2000) or cell signaling (Kadekaro et al., 2003a,b; Choi et al., 2006) at low concentrations, resulting in an increase in *TYR* and *TYRP2* mRNA. At concentrations of 50 and 100 μM, the levels of *TYR* and *TYRP2* mRNA and protein expression were closely correlated. Reduction in tyrosinase and DCT mRNA could account for reduced pigmentation in melanogenesis.

2.7. Kinetic analysis of mushroom tyrosinase

To examine their mechanism of action, 3-hydroxyphloretin (**7**) and catechol (**9**) were tested in a tyrosinase assay. 3-Hydroxyphloretin (**7**) exhibited a dose-dependent inhibitory effect on mushroom tyrosinase activity; the IC_{50} value was 63.4 μM. Furthermore, we performed an enzyme kinetics study of 3-hydroxyphloretin (**7**) with various concentrations of the L-tyrosine substrate (15.625, 31.25, 62.5, 125, 250, 500 μM). A Lineweaver–Burk plot of the data are shown in Fig. 6. The results indicate that 3-hydroxyphloretin (**7**) acted as a competitive inhibitor with respect to the substrate L-tyrosine. K_m and V_{max} val-

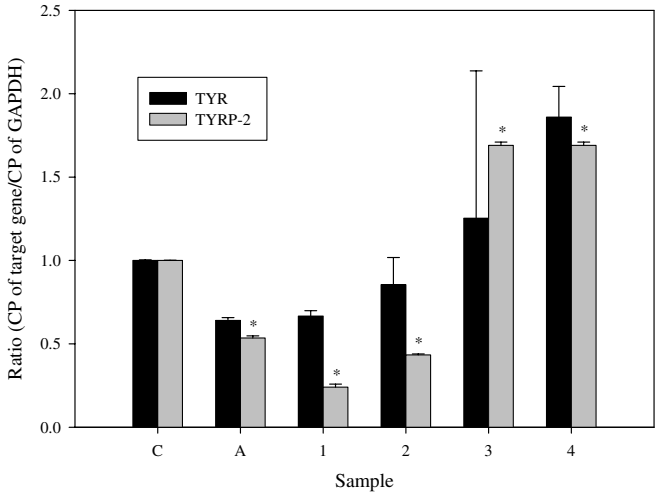

Fig. 5. Expression of *TYR* and *TYRP2* mRNAs in catechol (**9**)-treated human epidermal melanocytes (HEMn). The expression levels were normalized to the expression of GAPDH mRNA. Measurements were conducted in triplicate and the mean expression values for test samples relative to mean expression values for negative controls are indicated. (C) Medium only; (A) 3.0 mM arbutin; 1, 100 μM; 2, 50 μM; 3, 25 μM; 4, 10 μM. Data sets were determined to be significantly different using the non-parametric Mann–Whitney *U*-test ($p < 0.5$).

ues were calculated to be 3.9×10^{2} μM and 1.7×10^{-2} μM/min, respectively, for no inhibitor and 1.8×10^{3} μM and 1.2×10^{-2} μM/min, respectively, for 3-hydroxyphloretin (**7**). Catechol (**9**) exhibited no effect in this *in vitro* mushroom tyrosinase assay. This may be because the structure of catechol (**9**) is similar to an intermediate in melanin synthesis (Li et al., 2005). When we only added catechol (**9**) in the assay system without the substrate, L-tyrosine, 27% end product was produced; catechol (**9**) may act as a substrate in this *in vitro* enzyme assay. Thus, the results were different between the mushroom tyrosinase and HEMn cell-based tyrosinase assays. Obviously, *in vitro* activity in a mushroom tyrosinase assay does not necessarily predict in vivo performance on human skin. There are many factors involved, including cell membrane penetrability of constituents and different regulatory mechanisms in mammalian cells (Parvez et al., 2006).

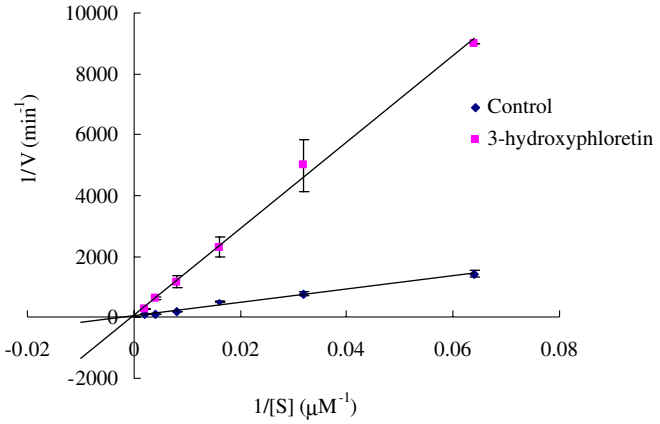

Fig. 6. Inhibitory effects of 3-hydroxyphloretin (**7**) (IC_{50} values) on mushroom tyrosinase. Lineweaver–Burk plots in the absence (control) and in the presence of test samples with L-tyrosine as the substrate.

2.8. Molecular docking study

In the literature, it is assumed that many tyrosinase inhibitors act by complexing the two copper ions, present in the active site of the enzyme (Sanchez-Ferrer et al., 1995). To explore potential binding interactions of 3-hydroxyphloretin (**7**) and catechol (**9**) with human tyrosinase, we carried out molecular docking studies with a focus on the di-copper binding site. As there are no experimental three-dimensional structures available for human tyrosi-

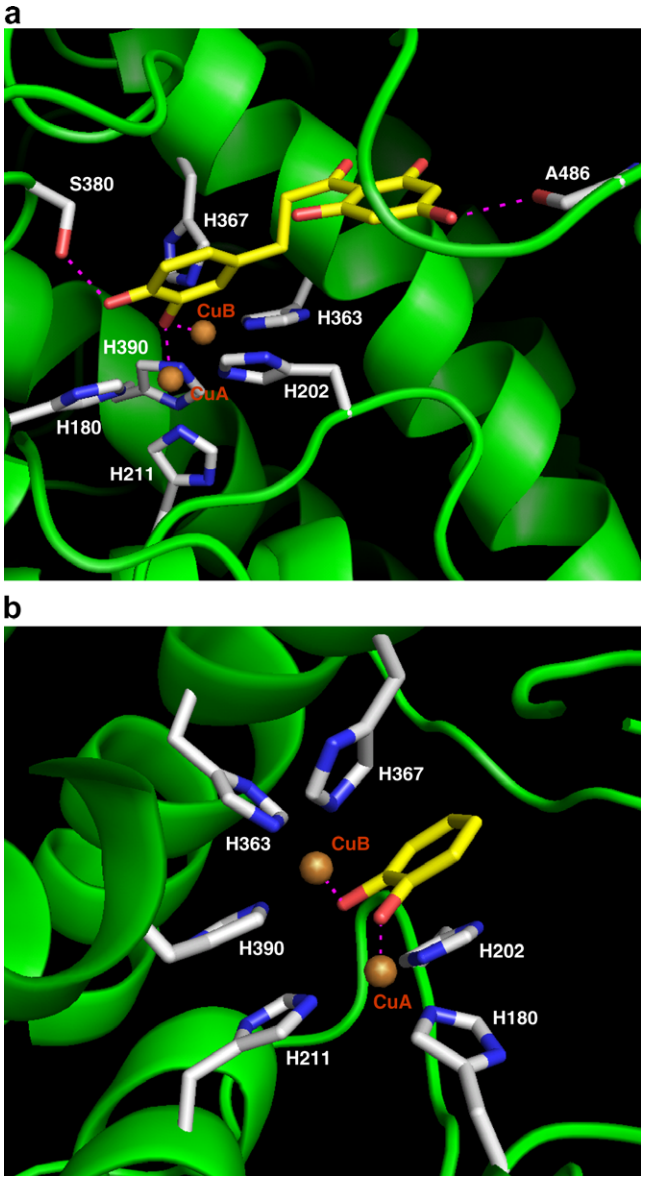

Fig. 7. The proposed binding modes of 3-hydroxyphloretin (**7**) (a) and catechol (**9**) (b) in the active site of human tyrosinase. The inhibitor molecules are colored in yellow for carbon atoms. The dashed lines show hydrogen-bonding or metal-coordination interactions. The docking models were generated using the AutoDock program and optimized by MD simulation and energy minimization.

nase, a theoretical homology model was retrieved from the ModBase database for the present docking study. To build a model with an active site in the probable ligand-bound conformation, a homology model was first simulated by complexing with the substrate L-DOPA and two copper ions, using molecular dynamics simulation and energy minimization (using the Tripos force field implemented in the SYBYL 7.1 package). We then carried out docking studies with 3-hydroxyphloretin (**7**) and catechol (**9**) in the active site of human tyrosinase with the AutoDock 3.0 program that can perform flexible-ligand docking using the LGA algorithm. The proposed favorable binding orientations of 3-hydroxyphloretin (**7**) and catechol (**9**), each with the lowest binding free energy estimated by AutoDock, are shown in Fig. 7. As shown in Fig. 7a, the two hydroxyl groups of 3-hydroxyphloretin (**7**) can form hydrogen bonds with residues Ser380 and Ala486. Importantly, one of the *ortho*-dihydroxyl groups in 3-hydroxyphloretin (**7**) makes metal-coordination interactions with the copper ions. Such coordination interactions are consistent with key binding interactions between monophenol or *ortho*-diphenol oxidases and their phenol substrates (Matoba et al., 2006). In contrast, catechol (**9**) has a smaller molecular size and can thus orient both of the *ortho*-dihydroxyl groups to coordinate with the copper ions (Fig. 7b). Based on these models, we suggest that the reduced effect of 3-hydroxyphloretin (**7**) and catechol (**9**) on human tyrosinase may be because they bind the active site as indicated by AutoDock.

3. Conclusions

In this study, 13 compounds isolated from the Formosan apple were characterized and evaluated for their hydroxyl-radical scavenging activity and cellular tyrosinase inhibitory activity in HEMn. Among the isolated constituents, 3-hydroxyphloretin (**7**) and catechol (**9**) are potentially the most interesting. Both 3-hydroxyphloretin (**7**) and catechol (**9**) reduced cellular tyrosinase activity in HEMn. Compared with the positive control, arbutin, these two compounds were about 50 times more potent in HEMn cells. 3-Hydroxyphloretin (**7**) also caused marginal (~20%) reduction (at 100 μM) in cell viability and had a marginal (~20%) reducing effect on melanin content. Catechol (**9**) affected the level of TRP-2 proteins and related gene expression at 50 and 100 μM. Thus, the reduction in the melanin formation by 3-hydroxyphloretin (**7**) and catechol (**9**) may not be due to direct tyrosinase inhibition, but because of effects on cell viability and toxicity. The two active compounds could also interact with the di-copper binding site of tyrosinase, based on molecular docking studies. The reduction of tyrosinase activity by these compounds may be because they act as substrates for tyrosinase and compete with the substrate for the tyrosinase active site (Khatib et al., 2005). These two compounds, isolated from the Formosan apple, may be useful as cosmetic agents to stimulate skin whitening.

4. Experimental

4.1. Materials and chemicals

A voucher specimen (M-38) of Formosan apple (*M. doumeri* var. *formosana*) was deposited at the Graduate Institute of Pharmacognosy (Taipei Medical University, Taipei, Taiwan). Luminol (5-amino-2,3-dihydro-1,4-phthalazinedione), potassium dihydrogenphosphate (KH_2PO_4), dipotassium hydrogen phosphate (K_2HPO_4), ethylenediaminetetraacetic acid (EDTA), ferric chloride ($FeCl_3$), and hydrogen peroxide (H_2O_2) were purchased from Sigma-Aldrich Chemical Co. (St. Louis, MO.). All chemicals and reagents used in the study were high-grade commercial products.

4.2. Extraction and isolation of constituents

Seven phenolic compounds, including phloretin (**1**), phloridzin (**2**), 3-hydroxyphloridzin (**3**), quercetin (**4**), chrysin (**5**), chrysin-5-glucoside (**6**), and 3-hydroxyphloretin (**7**), were isolated from Formosan apple as previously described (Leu et al., 2006). Except for those seven compounds, we isolated additional compounds from both the EtOAc and aqueous extracts. Briefly, dried leaves (560 g) were extracted with 70% aqueous acetone, three times at room temperature. The aqueous acetone extract was concentrated under reduced pressure and a suspension of the extract in H_2O was partitioned with EtOAc rendering an EtOAc and aqueous fraction. From the EtOAc extract, pynosylvin (**11**) (Schultz et al., 1992) was isolated using Sephadex LH-20 eluted with MeOH and chromatographed by semi-preparative HPLC (Biosil 5 ODS-W column, 4.6 × 250 mm; solvent system: H_2O:MeOH = 40:60; flow rate: 3.0 ml/min; detector: 254 nm). Oleanolic acid (**12**) and ursolic acid (**13**) (Budzikiewicz et al., 1963) were also purified from the EtOAc layer by using Sephadex LH-20 eluted with MeOH and silica gel eluted with CH_2Cl_2–acetone gradient, then subjected to further chromatography by semi-preparative HPLC with CH_3CN–H_2O (9:1, %) as eluent. The aqueous layer was also subjected to a Diaion HP 20 column using an elution with increasing MeOH concentrations. Seven fractions (1–7) were collected. Fraction 1 was subjected to semi-preparative HPLC (Biosil 5 ODS-W column, 4.6 × 250 mm; solvent system: H_2O:MeOH = 70:30; flow rate: 3.0 ml/min; detector: 254 nm) to obtain protocatechuic acid (**8**) (An et al., 2006) and catechol (**9**) (Webb and Ruszkay, 1998). Fraction 4 was re-purified using Toyopearl HW 40 with gradient MeOH (40% to 100% MeOH) and further purified with semi-preparative HPLC to obtain rutin (**10**) (Hou et al., 2005). Their structural identification were based on the physical and spectroscopic data reported in the literature. The purity of all isolated constituents was >98% as determined by the integration of proton resonances and diode array detection HPLC.

4.3. Measurement of hydroxyl radical using chemiluminescent (CL) reaction

Hydroxyl radicals were generated by the Fenton reaction using the modified luminescence method (Cheng et al., 2003). The reaction mixture contained 40 μM luminol, 4.17 mM phosphate buffer (pH 7.5), 4.6 μM Fe(II)-2.3 μM EDTA, test preparation, and 96 mM H_2O_2. The chemiluminescent reaction was carried out in KH_2PO_4–NaOH–buffered solution (pH 7.5) at room temperature. Initiation of the reaction was achieved by adding Fe(II)–EDTA followed by the addition of H_2O_2 into the mixture. The luminescence intensity was monitored within the wavelength range of 200–900 nm.

4.4. Cell culture

Primary skin melanocyte cells from neonatal foreskin (HEMn; Cascade Biologics Inc., Portland, OR) were cultured in Medium 254 (Cascade Biologics Inc.) supplemented with Human Melanocyte Growth Supplement (HMGS; Cascade Biologics Inc.).

4.5. MTT assay for cell viability

Cells were plated at 10^5/well (24-well plates). Twenty four hour after plating, test samples were added and cultures were incubated for an additional 24 h. Viability was determined using the 3-(4,5-dimethyl-thiazol-2-yl)-2,5-diphenyl tetrazolium bromide (MTT) method, a colorimetric assay based on the formation of purple formazan by mitochondrial dehydrogenase in active mitochondria.

4.6. Assay of cellular tyrosinase activity

The tyrosinase activity was measured using a slightly modified protocol (Nagata et al., 2004). Briefly, HEMn cells were cultured in 24-well plates. After treatment with individual test samples for 24 h, the cells were washed with PBS and lysed with phosphate buffer (pH 6.8) containing 1% Triton X-100. The cells were disrupted by freezing and thawing, with lysates were clarified by centrifugation at 10,000*g* for 10 min. After determining the protein content with a Bio-Rad protein assay kit, lysates were adjusted with lysis buffer to contain equal amounts of protein. These lysates were then added to wells (96-well plates) containing 2.5 mM L-DOPA in 0.1 M phosphate buffer (pH 6.8). After incubation at 37 °C for 1 h, the absorbance of samples was measured at 475 nm using an ELISA reader.

4.7. Measurement of melanin contents of melanocytes

Melanin contents was measured as described previously with minor modifications (Nagata et al., 2004). Cells were treated with test substances for 24 h and then harvested by centrifugation. Cell pellets were incubated in 1 N NaOH at 37 °C for 16 h and suspensions were clarified by centrifugation for 10 min at 10,000*g*. The optical densities (OD) of the supernatants were measured at 450 nm using an ELISA reader.

4.8. Western blot analysis

Western blot analyses to determine the extent of expression of tyrosinase and the TRPs were performed as described (Lee and Kang, 2003). Cells (10^6/well; 6-well plate) were lysed with PBS containing 1% Triton X-100, 1 mM phenylmethylsulfonyl fluoride (PMSF), 1 mg/ml aprotinin, and 10 mg/ml leupeptin, and lysates were subjected to centrifugation at 12,000*g* for 10 min. The total protein content of each supernatant was determined with a Bio-Rad protein assay kit. An equal amount of protein of each sample was added to sodium dodecyl sulfate sample buffer and proteins were separated by polyacrylamide gel (10%) electrophoresis. Following electrotransfer to PVDF membranes (Immobilon-P, Millipore Corp., Bedford, MA), the membranes were incubated overnight with PBS containing 5% non-fat dry milk, 0.1% Tween 20, and 0.1% NaN_3. Anti-tyrosinase (C-19), anti-TRP1 (G-17), and anti-TRP2 (D-18) antibodies (Santa Cruz Biotechnology Inc., CA, USA) were added at a 1:1000 dilution, and membranes were incubated at room temperature for 3 h. After extensive washes, the blots were incubated for 2 h at room temperature with alkaline phosphatase-conjugated anti-goat IgG (Santa Cruz Biotechnology) diluted 1:5000 in PBS containing 5% non-fat dry milk, 0.1% Tween 20, and 0.1% NaN_3. After washing, protein-bound alkaline phosphatase activity was detected with nitro blue tetrazolium (NBT)/5-bromo-4-chloro-3-indolyl phosphate (BCIP) substrate. The extent of protein loading was evaluated by Western blotting using a β-actin antibody.

4.9. RNA extraction and reverse transcription

Total RNA was extracted using the High Pure RNA Isolation Kit (Roche Molecular Biochemicals, Mannheim, Germany). The quality of the total RNA sample was evaluated by determination of the OD_{260}/OD_{280} ratio. To prepare a cDNA pool from each RNA sample, total RNA (1 μg) was reverse transcribed using the Transcriptor First Strand cDNA Synthesis Kit (Roche) according to the manufacturer's instructions. Each cDNA pool was stored at −20 °C until real-time PCR analysis was performed.

4.10. PCR primers

Specific oligonucleotide primer pairs to be used for quantitative real-time PCR (q-RT PCR) were selected from the Roche Universal ProbeLibrary. The sequences of the primers used are as follows: *TYR* forward primer: CATTCTTCTCCTCTTGGCAGA and *TYR* reverse primer:

CCGCTATCCCAGTAAGTGGA; *TYRP1* forward primer: GCTTTTCTCACATGGCACAG and *TYRP1* reverse primer: GGCTCTTGCAACATTTCCTG; *TYRP2* forward primer: CGACTCTGATTAGTCGGAACTCA and *TYRP2* reverse primer: GGTGGTTGTAGTCATCCAAGC; *GAPDH* forward primer: AGCCACATCGCTCAGACAC and *GAPDH* reverse primer: GCCCAATACGACCAAATCC.

4.11. Quantitative real-time PCR

Quantitative real-time PCR reactions were performed on the Roche LightCycler Instrument 2.0 using LightCycler® TaqMan Master (Roche). ProbeFinder software (http://www.universalprobelibrary.com) was used to design the optimal assay comprised of the respective labeled probe of the Universal ProbeLibrary Set and human and gene-specific primers. Briefly, 20 μl reaction mixtures contained 5 μl cDNA template, 4 μl Master Mix, 10 μM probe (0.2 μl), 10 μM forward primer (0.4 μl), 10 μM reversed primer (0.4 μl), and 10 μl water. The RT-PCR program was 95 °C for 10 min, 45 cycles of 95 °C for 10 s, 72 °C for 1 s, and 40 °C for 30 s. At the end of the program a melt curve analysis was performed. The data of each RT-PCR run were automatically analyzed and an amplification plot was generated for each cDNA sample. From each of these plots, the LightCycler4 Data Analysis Software automatically calculates the CP value (crossing point: the turning point corresponds to the first maximum of the second derivative curve) which indicates the beginning of exponential amplification. The mRNA level was normalized with reference to the amount of housekeeping gene transcript (*GAPDH* mRNA).

4.12. Mushroom tyrosinase purified enzyme assay

Mushroom tyrosinase activity was measured by a method modified from that of Pomerantz (Masuda et al., 2005). Mushroom tyrosinase was reconstituted in 0.4 M HEPES buffer, pH 6.8, at 5000 U/ml and stored at −20 °C prior to use. The reaction mixture consisted of 250 μM L-tyrosine, 50 U/ml mushroom tyrosinase, and test sample. After incubation for 30 min at 37 °C, the absorbance was measured at 475 nm in a model μQuant microplate reader (Bio-tek Instruments, Inc.).

4.13. Assessment of mushroom tyrosinase inhibition kinetics

The assays were carried out with the IC_{50} values of tested samples and various concentrations (15.625, 31.25, 62.5, 125, 250, and 500 μM) of substract, L-tyrosine. The apparent inhibition constants (K_m) for the compounds were calculated by Lineweaver–Burk plots for the tested samples by, respectively, plotting the slope of each double reciprocal plot versus the corresponding inhibitor concentration at which it was obtained (Huang et al., 2006).

4.14. Molecular modeling

An available 3D model of human tyrosinase, computed by homology modeling based on the X-ray crystal structure of hemocyanin (PDB code 1JS8), was retrieved from the ModBase database (Pieper et al., 2004). With the use of this theoretical model, two copper ions and the substrate L-DOPA were manually positioned into the active site of the enzyme. The complex structure was simulated using the software package SYBYL 7.1 (Tripos, Inc., St. Louis, MO) in order to build a model whose active site exists in the probable ligand-bound conformation. The initial simulation was performed with 100 cycles each of steepest descent and conjugate gradient minimization by relaxing ligands and the six histidine residues involved in the copper ion binding (H180, H202, H211, H363, H367, and H390), while keeping the rest of the complex fixed. For the resulting structure, two structural subsets A and B were then defined as the residues farther than 10 Å from the two copper ions and the rest of the complex, respectively. The simulations were accomplished through the following sequential steps: (i) 200 cycles each of steepest descent and conjugate gradient minimization by fixing subset A and the backbone atoms of subset B, (ii) 200 cycles of conjugate gradient minimization by fixing subset A, (iii) 3-ps molecular dynamics (MD) simulation (time step of 1 fs) at 300 K followed by conjugate gradient minimization to reach a convergence of 0.05 kcal/(mol Å) by fixing subset A and the backbone atoms of subset B, and (iv) conjugate gradient minimization to reach a convergence of 0.05 kcal/(mol Å) by fixing subset A. All calculations were performed with the Tripos force field, a distance-dependent dielectric constant of 1*r*, and a nonbonded cutoff of 12 Å.

The resulting structure obtained using the above simulations was used for docking studies with the AutoDock 3.0 program (The Scripps Research Institute, La Jolla, CA) (Morris et al., 1998). L-DOPA and nonpolar hydrogens were first removed from the complex, and the protein atoms were assigned with Kollman united-atom partial charges. The 3D structures of active compounds were generated and energy minimized with the Tripos force field in SYBYL. The partial atomic charges were calculated using the Gasteiger–Marsili method. The flexible torsions for compounds were defined with AutoTors implemented in the AutoDock program. To carry out docking simulations, a grid box was defined to enclose the dicopper binding site with dimensions of $26.3 \times 26.3 \times 26.3$ Å and a grid spacing of 0.375 Å. The grid maps for energy scoring were calculated using AutoGrid. Docking was performed using the Lamarckian genetic algorithm (LGA) and the pseudo-Solis and Wets local search method. Default parameters were used except for energy evaluations (5×10^5) and docking runs (50). The obtained docked model with the predicted lowest binding free energy for each compound was then subjected to geometry optimization in SYBYL. By fixing the residues father than 6 Å from the inhibitor, the geometry optimization was achieved by 200 cycles each

of steepest descent and conjugate gradient minimization, 3-ps MD simulation (time step of 1 fs) at 300 K, and finally conjugate gradient minimization to reach a convergence of 0.05 kcal/(mol Å). In the present study, all computer simulations were performed on the Silicon Graphics Origin 3800 system and an Octane workstation.

4.15. Statistical analysis

Differences between the data sets were tested for significance by means of the non-parametric Mann–Whitney *U*-test. $p < 0.5$ was considered to indicate significantly different data sets.

Acknowledgements

This work was supported in part by financial support from the Juridical Person of Yen's Foundation (Taiwan). We also thank the National Center for High-Performance Computing (NCHC, in Hsinchu, Taiwan) for providing computing resources.

References

Abdel-Malek, Z., Swope, V., Collins, C., Boissy, R., Zhao, H., Nordlund, J., 1993. Contribution of melanogenic proteins to the heterogeneous pigmentation of human melanocytes. Journal of Cell Science 106, 1323–1331.

Abdel-Malek, Z.A., Swope, V.B., Nordlund, J.J., Medrano, E.E., 1994. Proliferation and propagation of human melanocytes *in vitro* are affected by donor age and anatomical site. Pigment Cell Research 7, 116–122.

An, L.J., Guan, S., Shi, G.F., Bao, Y.M., Duan, Y.L., Jiang, B., 2006. Protocatechuic acid from *Alpinia oxyphylla* against MPP(+)-induced neurotoxicity in PC12 cells. Food and Chemical Toxicology 44, 436–443.

Bergamini, C.M., Gambetti, S., Dondi, A., Cervellati, C., 2004. Oxygen, reactive oxygen species and tissue damage. Current Pharmaceutical Design 10, 1611–1626.

Briganti, S., Camera, E., Picardo, M., 2003. Chemical and instrumental approaches to treat hyperpigmentation. Pigment Cell Research 16, 101–110.

Budzikiewicz, J.M., Wilson, J.M., Djerassi, C., 1963. Mass spectrometry in structural and stereochemical problems. XXXII. Pentacyclic triterpenes. Journal of the American Chemical Society 85, 3688–3699.

Cheng, Z., Yan, G., Li, Y., Chang, W., 2003. Determination of antioxidant activity of phenolic antioxidants in a Fenton-type reaction system by chemiluminescence assay. Analytical and Bioanalytical Chemistry 375, 376–380.

Choi, Y.G., Bae, E.J., Kim, D.S., Park, S.H., Kwon, S.B., Na, J.I., Park, K.C., 2006. Differential regulation of melanosomal proteins after chinokitiol treatment. Journal of Dermatological Science 43, 181–188.

Eberle, A.N., Bodi, J., Orosz, G., Suli-Vargha, H., Jaggin, V., Zumsteg, U., 2001. Antagonist and agonist activities of the mouse agouti protein fragment (91–131) at the melanocortin-1 receptor. Journal of Receptor and Signal Transduction Research 21, 25–45.

Fang, D., Tsuji, Y., Setaluri, V., 2002. Selective down-regulation of tyrosinase family gene TYRP1 by inhibition of the activity of melanocyte transcription factor, MITF. Nucleic Acids Research 30, 3096–3106.

Halaban, R., Pomerantz, S.H., Marshall, S., Lambert, D.T., Lerner, A.B., 1983. Regulation of tyrosinase in human melanocytes grown in culture. Journal of Cell Biology 97, 480–488.

Harman, D., 2003. The free radical theory of aging. Antioxidants & Redox Signaling 5, 557–561.

Hearing, V.J., 1999. Biochemical control of melanogenesis and melanosomal organization. Journal of Investigative Dermatology Symposium Proceedings 4, 24–28.

Hearing, V.J., 2005. Biogenesis of pigment granules: a sensitive way to regulate melanocyte function. Journal of Dermatological Science 37, 3–14.

Hirobe, T., 2005. Role of keratinocyte-derived factors involved in regulating the proliferation and differentiation of mammalian epidermal melanocytes. Pigment Cell Research 18, 2–12.

Hou, W.C., Lin, R.D., Lee, T.H., Huang, Y.H., Hsu, F.L., Lee, M.H., 2005. The phenolic constituents and free radical scavenging activities of *Gynura formosana* Kiamnra. Journal of the Science of Food and Agriculture 85, 615–621.

Houghton, A.N., 1994. Cancer antigens: immune recognition of self and altered self. Journal of Experimental Medicine 180, 1–4.

Huang, X., Chen, Q., Wang, Q., Song, K., Wang, J., Sha, L., Guan, X., 2006. Inhibition of the activity of mushroom tyrosinase by alkylbenzoic acids. Food Chemistry 94, 1–6.

Kadekaro, A.L., Kanto, H., Kavanagh, R., Abdel-Malek, Z.A., 2003a. Significance of the melanocortin 1 receptor in regulating human melanocyte pigmentation, proliferation, and survival. Annals of the New York Academy of Sciences 994, 359–365.

Kadekaro, A.L., Kavanagh, R.J., Wakamatsu, K., Ito, S., Pipitone, M.A., Abdel-Malek, Z.A., 2003b. Cutaneous photobiology. The melanocyte vs. the sun: who will win the final round? Pigment Cell Research 16, 434–447.

Kao, M.T., 1996. In: Kao, M.T. (Ed.), Popular Herbal Rededies of Taiwan (3). SMC Publishing Inc., Taipei, p. 54.

Khatib, S., Nerya, O., Musa, R., Shmuel, M., Tamir, S., Vaya, J., 2005. Chalcones as potent tyrosinase inhibitors: the importance of a 2,4-substituted resorcinol moiety. Bioorganic and Medicinal Chemistry 13, 433–441.

Kim, Y.J., Uyama, H., 2005. Tyrosinase inhibitors from natural and synthetic sources: structure, inhibition mechanism and perspective for the future. Cellular and Molecular Life Sciences 62, 1707–1723.

Kim, D., Park, J., Kim, J., Han, C., Yoon, J., Kim, N., Seo, J., Lee, C., 2006. Flavonoids as mushroom tyrosinase inhibitors: a fluorescence quenching study. Journal of Agricultural & Food Chemistry 54, 935–941.

Kushimoto, T., Basrur, V., Valencia, J., Matsunaga, J., Vieira, W.D., Ferrans, V.J., Muller, J., Appella, E., Hearing, V.J., 2001. A model for melanosome biogenesis based on the purification and analysis of early melanosomes. Proceedings of the National Academy of Sciences of the United States of America 98, 10698–10703.

Kushimoto, T., Valencia, J.C., Costin, G.E., Toyofuku, K., Watabe, H., Yasumoto, K., Rouzaud, F., Vieira, W.D., Hearing, V.J., 2003. The Seiji memorial lecture: the melanosome: an ideal model to study cellular differentiation. Pigment Cell Research 16, 237–244.

Lee, J.Y., Kang, W.H., 2003. Effect of cyclosporin A on melanogenesis in cultured human melanocytes. Pigment Cell Research 16, 504–508.

Leu, S.J., Lin, Y.P., Lin, R.D., Wen, C.L., Cheng, K.T., Hsu, F.L., Lee, M.H., 2006. Phenolic constituents of *Malus doumeri* var. *formosana* in the field of skin care. Biological and Pharmaceutical Bulletin 29, 740–745.

Li, C.Y., Gao, T.W., Wang, G., Han, Z.Y., Shen, Z., Li, T.H., Liu, Y.F., 2004. The effect of antisense tyrosinase-related protein 1 on melanocytes and malignant melanoma cells. British Journal of Dermatology 150, 1081–1090.

Li, N., Xue, M.H., Yao, H., Zhu, J.J., 2005. Reagentless biosensor for phenolic compounds based on tyrosinase entrapped within gelatine film. Analytical and Bioanalytical Chemistry 383, 1127–1132.

Maeda, K., Yokokawa, Y., Hatao, M., Naganuma, M., Tomita, Y., 1997. Comparison of the melanogenesis in human black and light brown melanocytes. Journal of Dermatological Science 14, 199–206.

Masuda, T., Yamashita, D., Takeda, Y., Yonemori, S., 2005. Screening for tyrosinase inhibitors among extracts of seashore plants and

identification of potent inhibitors from *Garcinia subelliptica*. Bioscience, Biotechnology & Biochemistry 69, 197–201.

Matoba, Y., Kumagai, T., Yamamoto, A., Yoshitsu, H., Sugiyama, M., 2006. Crystallographic evidence that the dinuclear copper center of tyrosinase is flexible during catalysis. Journal of Biological Chemistry 281, 8981–8990.

Morris, G.M., Goodsell, D.S., Halliday, R.S., Huey, R., Hart, W.E., Belew, R., 1998. Automated docking using a Lamarckian genetic algorithm and an empirical binding free energy function. Journal of Computational Chemistry 19, 1639–1662.

Nagata, H., Takekoshi, S., Takeyama, R., Homma, T., Yoshiyuki Osamura, R., 2004. Quercetin enhances melanogenesis by increasing the activity and synthesis of tyrosinase in human melanoma cells and in normal human melanocytes. Pigment Cell Research 17, 66–73.

Negroiu, G., Dwek, R.A., Petrescu, S.M., 2000. Folding and maturation of tyrosinase-related protein-1 are regulated by the post-translational formation of disulfide bonds and by *N*-glycan processing. Journal of Biological Chemistry 275, 32200–32207.

Oetting, W.S., 2000. The tyrosinase gene and oculocutaneous albinism type 1 (OCA1): A model for understanding the molecular biology of melanin formation. Pigment Cell Research 13, 320–325.

Parvez, S., Kang, M., Chung, H.S., Cho, C., Hong, M.C., Shin, M.K., Bae, H., 2006. Survey and mechanism of skin depigmenting and lightening agents. Phytotherapy Research 20, 921–934.

Pieper, U., Eswar, N., Braberg, H., Madhusudhan, M.S., Davis, F.P., Stuart, A.C., Mirkovic, N., Rossi, A., Marti-Renom, M.A., Fiser, A., Webb, B., Greenblatt, D., Huang, C.C., Ferrin, T.E., Sali, A., 2004. MODBASE, a database of annotated comparative protein structure models, and associated resources. Nucleic Acids Research 32, D217–D222.

Reiter, R.J., Acuna-Castroviejo, D., Tan, D.X., Burkhardt, S., 2001. Free radical-mediated molecular damage. Mechanisms for the protective actions of melatonin in the central nervous system. Annals of the New York Academy of Sciences 939, 200–215.

Sanchez-Ferrer, A., Rodriguez-Lopez, J.N., Garcia-Canovas, F., Garcia-Carmona, F., 1995. Tyrosinase: a comprehensive review of its mechanism. Biochimica et Biophysica Acta 1247, 1–11.

Schultz, T.P., Boldin, W.D., Fisher, T.H., Nicholas, D.D., Mcmurtrey, K.D., Pobanz, K., 1992. Structure–fungicidal properties of some 3-and 4-hydroxylated stilbenes and bibenzyl analogues. Phytochemistry 31, 3801–3806.

Sturm, R.A., Box, N.F., Ramsay, M., 1998. Human pigmentation genetics: the difference is only skin deep. BioEssays 20, 712–721.

Tripathi, R.K., Hearing, V.J., Urabe, K., Aroca, P., Spritz, R.A., 1992. Mutational mapping of the catalytic activities of human tyrosinase. Journal of Biological Chemistry 267, 23707–23712.

Vijayasaradhi, S., Bouchard, B., Houghton, A.N., 1990. The melanoma antigen gp75 is the human homologue of the mouse b (brown) locus gene product. Journal of Experimental Medicine 171, 1375–1380.

Vijayasaradhi, S., Doskoch, P.M., Houghton, A.N., 1991. Biosynthesis and intracellular movement of the melanosomal membrane glycoprotein gp75, the human b (brown) locus product. Experimental Cell Research 196, 233–240.

Webb, K.S., Ruszkay, S.J., 1998. Oxidation of aldhydes with oxone in aqueous acetone. Tetrahedron 54, 401–410.

Westerhof, W., 2006. The discovery of the human melanocyte. Pigment Cell Research 19, 183–193.

Widlund, H.R., Fisher, D.E., 2003. Microphthalamia-associated transcription factor: a critical regulator of pigment cell development and survival. Oncogene 22, 3035–3041.

Yamakoshi, J., Otsuka, F., Sano, A., Tokutake, S., Saito, M., Kikuchi, M., Kubota, Y., 2003. Lightening effect on ultraviolet-induced pigmentation of guinea pig skin by oral administration of a proanthocyanidin-rich extract from grape seeds. Pigment Cell Research 16, 629–638.